Electronic Supplementary Material (ESI) for Journal of Materials Chemistry B.
This journal is © The Royal Society of Chemistry 2021

Electronic Supplementary Information for

Self-assembly gel-based dynamic response system for specific recognition of *N*-acetylneuraminic acid

Xue Wang,[ab] Shengxu Qian,[b] Dongdong Wang,[b] Cunli Wang,[b] Haijuan Qin,[c] Lang Peng,[b] Wenqi Lu,[b] Yahui Zhang[b] and Guangyan Qing*[bd]

[a]*State Key Laboratory of Advanced Technology for Materials Synthesis and Processing, Wuhan University of Technology, 122 Luoshi Road, Wuhan 430070, P. R. China.*

[b]*Key Laboratory of Separation Science for Analytical Chemistry, Dalian Institute of Chemical Physics, Chinese Academy of Sciences, 457 Zhongshan Road, Dalian 116023, P. R. China.*

[c]*Research Centre of Modern Analytical Technology, Tianjin University of Science and Technology, Tianjin 300457, P. R. China.*

[d]*College of Chemistry and Chemical Engineering, Wuhan Textile University, 1 Sunshine Road, Wuhan 430200, P. R. China.*

*Corresponding authors: qinggy@dicp.ac.cn

Instruments

1D Nuclear magnetic resonance (NMR) spectra were recorded on Bruker AVANCE III 400M NMR spectrometer (Bruker, Germany). 2D Nuclear magnetic resonance (NMR) spectra were recorded on an AVANCE III HD 700 MHz spectrometer (Bruker, Germany). Mass spectrum (MS) was obtained with a Quadrupole Time-of-Flight (Q-TOF) 6540 masshunter (Agilent, USA). Infrared spectra were recorded on a USA BioTools Chiral IR-2X spectrometer. X-ray diffraction (XRD) was conducted on a PANalytical X'Pert PRO X-ray (Philips, Japan) diffractometer with Cu *K*α radiation source (λ= 1.54059 Å). Fluorescence spectra were recorded on a PerkinElmer FL-6500 Fluorescence Spectrophotometer (PerkinElmer, USA). Helium ion microscopy (HIM) images were conducted on a ORION NANOFAB (Carl Zeiss, Germany). Atomic Force Microscopy (AFM) investigation was conducted on a NanoWizard Ultra Speed AFM (JPK, Germany) in a QI mode. Dynamic light scattering (DLS) measurement was monitored on a Malvern Zetasizer Nano ZS90 (Malvern, UK).

Synthesis and Characterization

Synthesis of L-PyHis

L-PyHis was synthetized through one-step reaction according to the reproted literature.[1] First, L-(+)-Histidine methyl ester dihydrochloride (2.0 g, 8.3 mmol) was dissolved in dry dichloromethane (250 mL), and added with triethylamine (2.1 g, 20.7 mmol). The mixture was stirred at room temperature for 1 h. Then 1-Pyrenecarboxylic acid (1.7 g, 6.9 mmol), 1-Hydroxybenzotriazole (HOBt) (1.2 g, 9.0 mmol) and 1-(3-Dimethylaminopropyl)-3-ethylcarbodiimide hydrochloride (EDC·HCl) (1.7 g, 9.0 mmol) were added to the solution, and the mixed solution was stirred at room temperature overnight. After that, the reaction mixture was washed three times (3 × 250 mL) with saturated $NaHCO_3$ aqueous solution. The organic phase was collected and dried with anhydrous Na_2SO_4. After filtration, the organic solvent was evaporated under reduced pressure and the residue was purified by silica gel column with an elution of dichloromethane and methanol and recrystallization. The final product was light yellow solid (1.7 g, 4.3 mmol, yield 62.3%).

Characterization data for L-PyHis: ^{1}H NMR (400 MHz, DMSO-d_6, 298K): δ (ppm): 11.93 (s, 1H), 9.10 (d, J = 7.2 Hz, 1H), 8.37-8.06 (m, 9H), 7.62 (s, 1H), 6.94 (s, 1H), 4.90 (m, 7.7 Hz, 1H), 3.75 (s, 3H), 3.09 (m, 9.7 Hz, 2H). ^{13}C NMR (400 MHz, DMSO-d_6, 298K): δ (ppm): 172.17, 168.95, 135.09, 133.62, 131.68, 131.28, 130.67, 130.16, 128.36, 128.09, 127.80, 127.17, 126.59, 125.82, 125.60, 125.13, 124.55, 124.38, 123.69, 123.55, 116.57, 53.22, 52.04, 28.64. MALDI-MS: m/z calcd. for $C_{24}H_{19}N_3O_3$: 397.14; found: 398.15 $[M+H]^+$. Elemental analysis calcd. (%) for $C_{24}H_{19}N_3O_3$: C, 72.53; H, 4.82; N, 10.57. Found: C, 72.65; H, 4.75; N, 10.60.

Helium ion microscopy and atom force microscopy experiments

First, the L-PyHis stock solution was diluted to 4 mM. Then, 0.02 mL L-PyHis ethanol solution was mixed with 0.08 mL aqueous solution of different saccharides (i.e., lactose, Neu5Ac, and 2,3'-Sialyllactose). The final concentrations of L-PyHis and various saccharides were both 0.8 mM. The saccharide aqueous solution was replaced by water in the blank experiment. Each sample was dropped onto the clear glass surface, and allowing them to dry in the air.

Figures

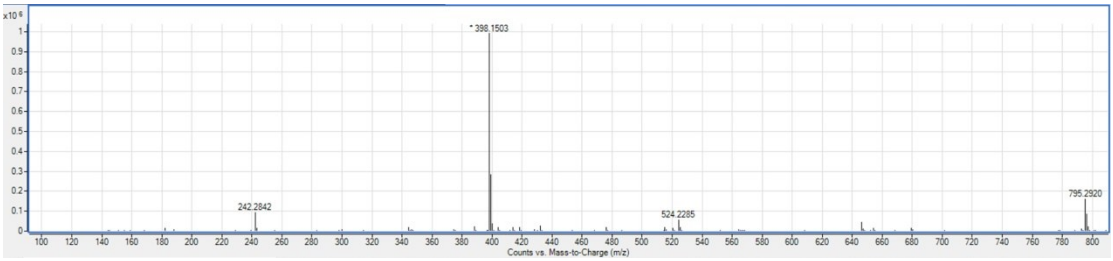

Fig. S1 The MS spectrum of L-PyHis.

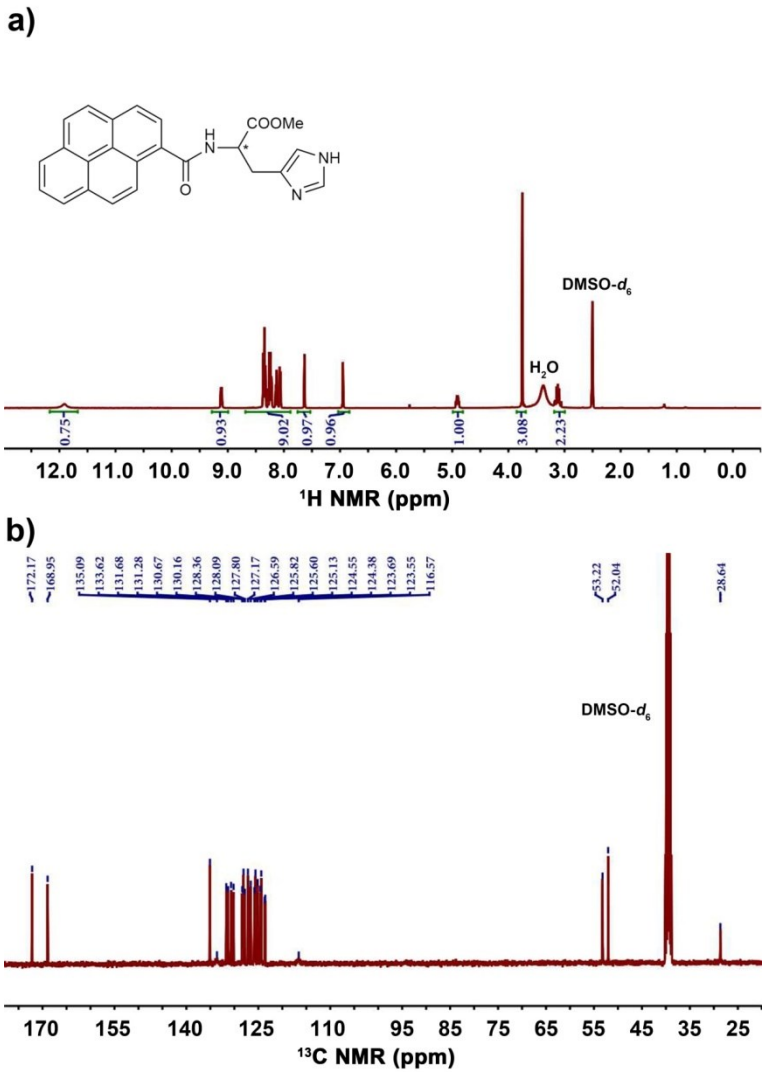

Fig. S2 ^{1}H (a) and ^{13}C NMR (b) spectra of L-PyHis in DMSO–d_6 at 20 °C.

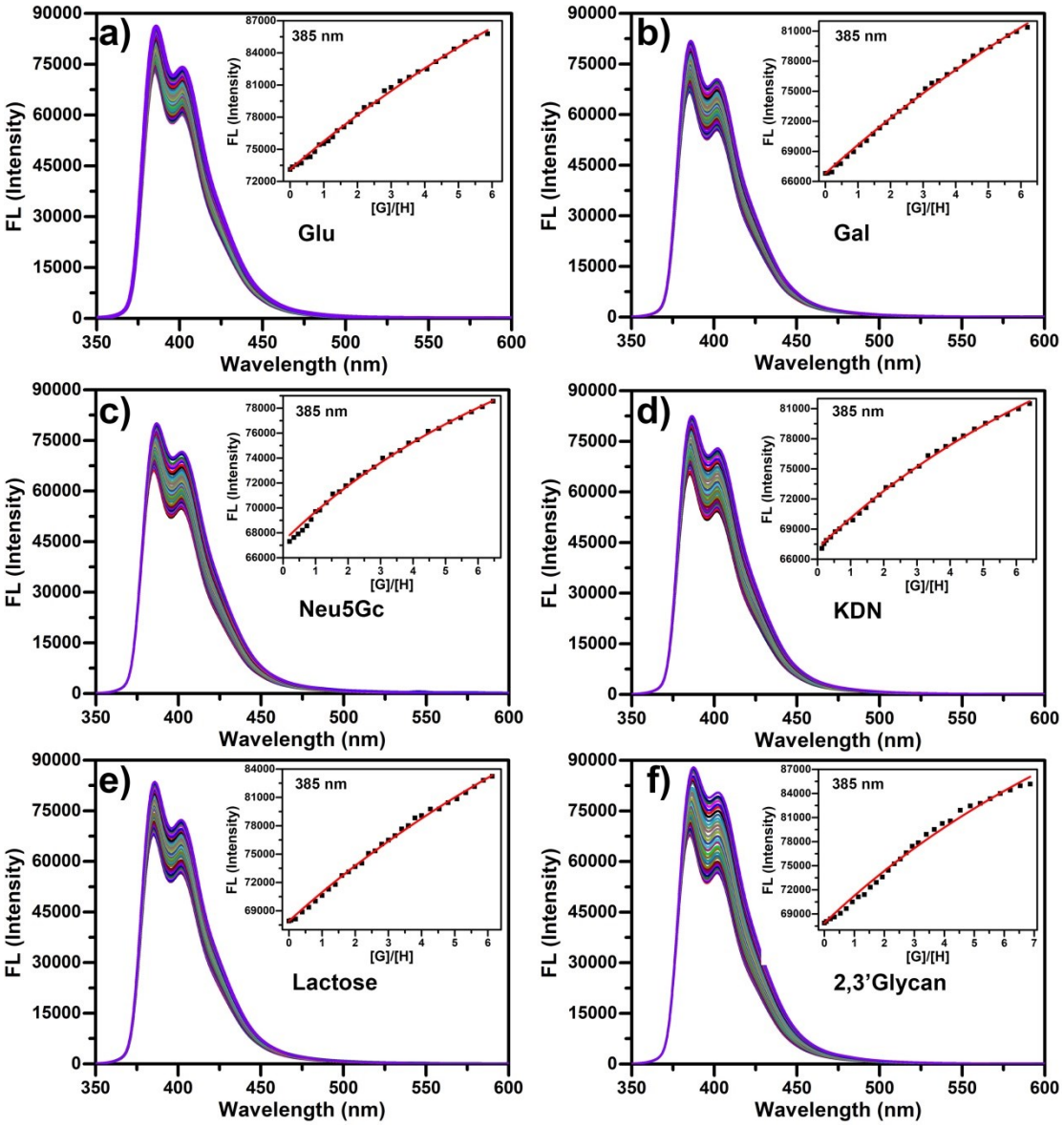

Fig. S3 Fluorescence spectra (λ_{ex}: 330 nm) of L-PyHis (1.0×10^{-5} mol·L^{-1}) upon additions of different equivalents of various saccharides solutions in water at 25 °C. Inset: The corresponding fluorescent intensity changes (λ_{em}: 385 nm) dependent on the molar ratios of guest to host. Red line denotes a nonlinear fitting curve. (a) Glu; (b) Gal; (c) Neu5Gc; (d) KDN; (e) lactose; (f) 2,3'-Sialyllactose. The association constant (K_a) of L-PyHis with Glu, Gal, Neu5Gc, KDN, lactose and 2,3'-Sialyllactose were are 4.3×10^3, 3.9×10^3, 8.1×10^3, 7.2×10^3, 4.7×10^3, and 5.5×10^3 L·mol^{-1} respectively.

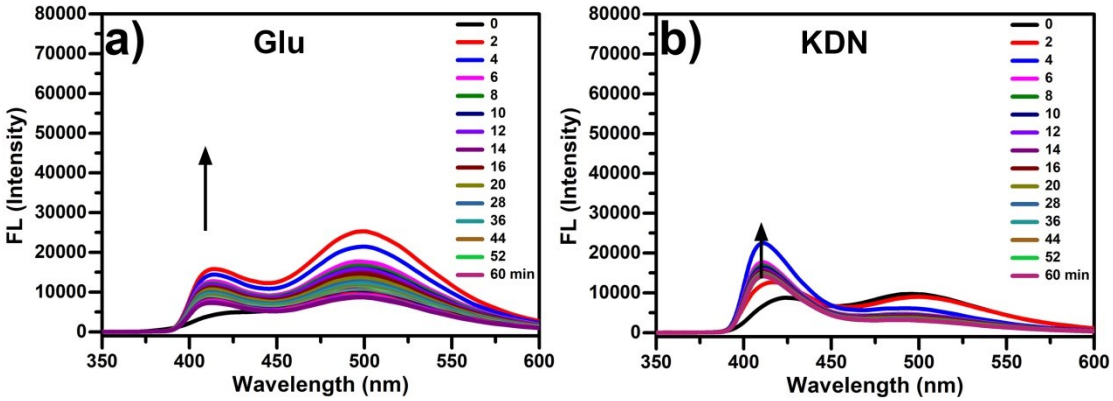

Fig. S4 Time dependence of fluorescence spectra changes of L-PyHis with the addition of Glu (a), KDN (b). The final concentrations of L-PyHis and various saccharides are 8 mM and 0.8 mM, respectively.

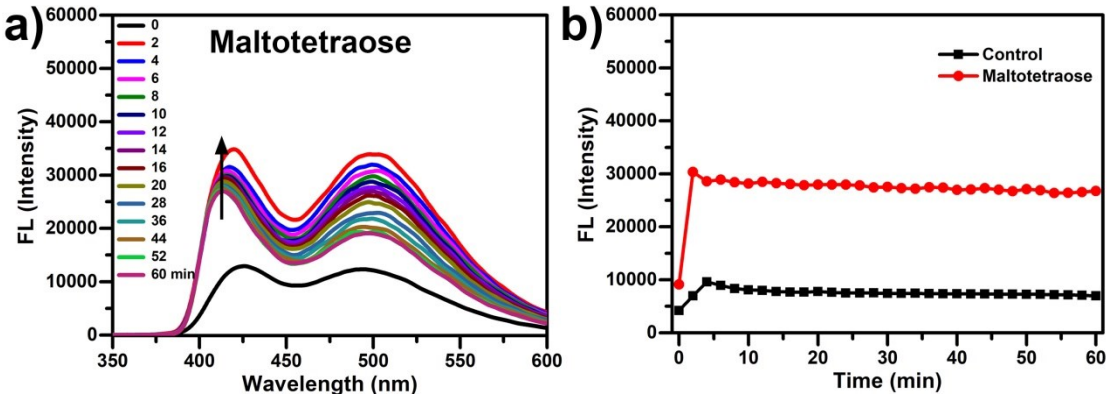

Fig. S5 (a) Time dependence of fluorescence spectra changes of L-PyHis with the addition of maltotetraose. (b) Time dependence of fluorescent intensity changes of L-PyHis at 410 nm after adding water or maltotetraose.

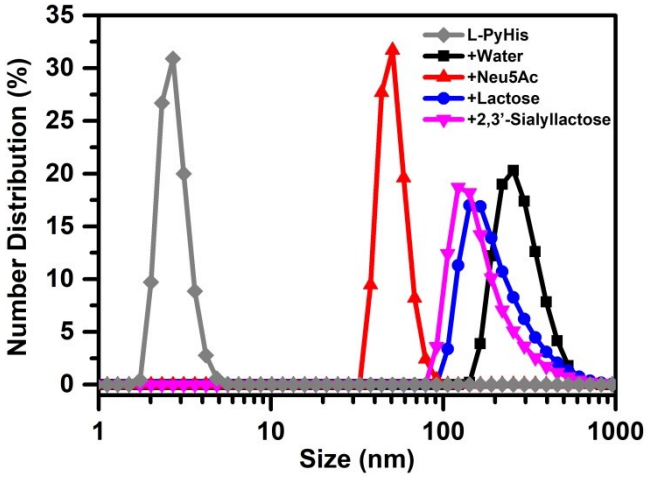

Fig. S6 The hydrodynamic diameter of L-PyHis before (gray) and after adding water (black), Neu5Ac (red), lactose (blue) or 2,3'-Sialyllactose (pink).

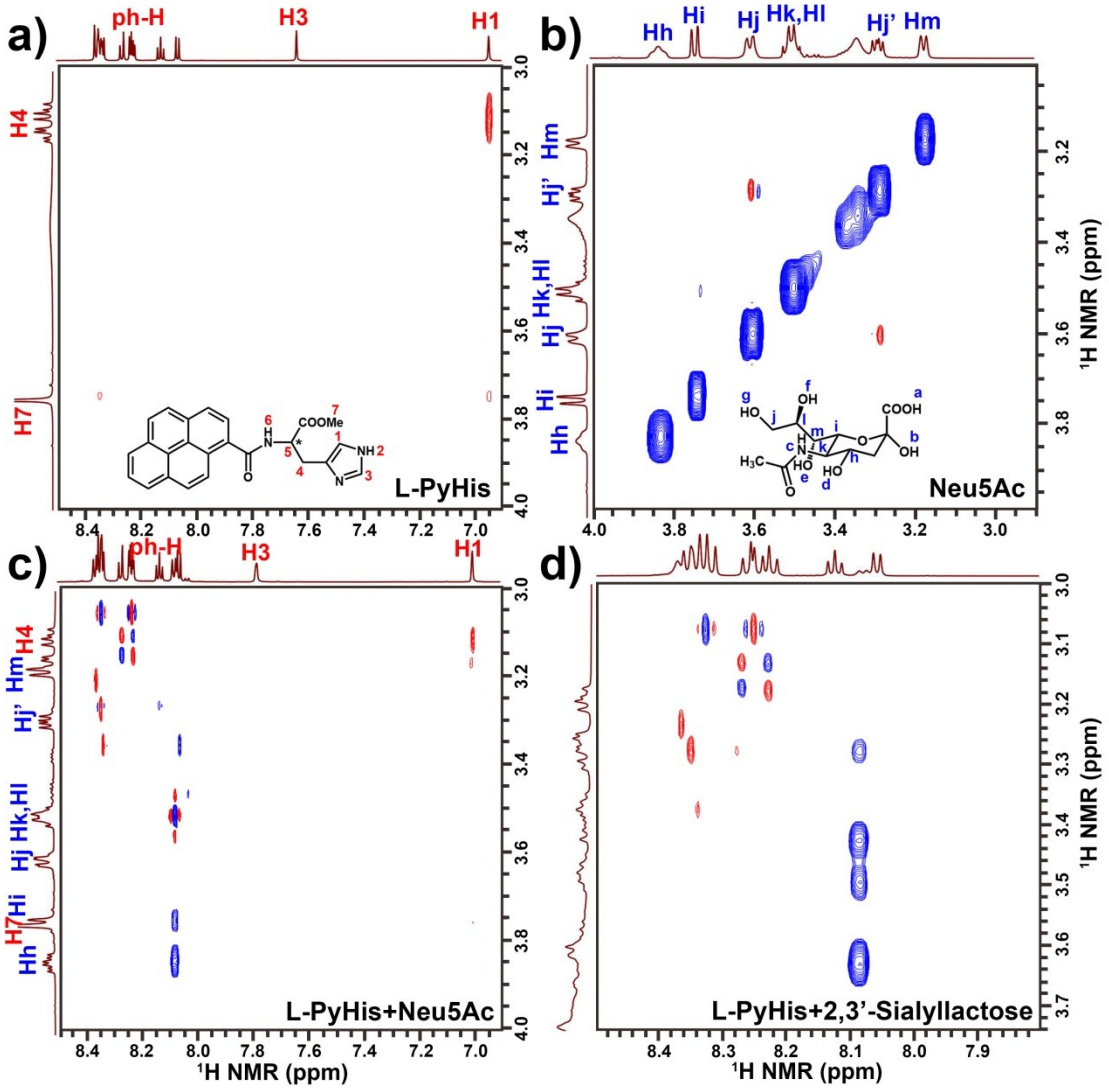

Fig. S7 Partial ^{1}H-^{1}H NOESY NMR spectrum of L-PyHis (a), Neu5Ac (b) and the mixture of L-PyHis with Neu5Ac (c) or 2,3'-Sialyllactose (d) at a molar ratio of 1:1 in d_6-DMSO at 20 °C. The concentrations of L-PyHis and saccharides were both 0.03 M.

Supplementary References

(1) D. Niu, Y. Q. Jiang, L. K. Ji, G. H. Ouyang, M. H. Liu, *Angew. Chem. Int. Ed.* 2019, **58**, 5946–5950.